Modern Environmental Science and Engineering (ISSN 2333-2581)
January 2016, Volume 2, No. 1, pp. 757-764
Doi: 10.15341/mese(2333-2581)/01.02.2016/008
Academic Star Publishing Company, 2016
www.academicstar.us

Determination of Radionuclides Surface Concentration and Radiation Level in Fukushima Prefecture, Japan

Godwin Ekong, Isa Sambo, and Saiyadi Sulaiman
Nigerian Nuclear Regulatory Authority, Nigeria

Abstract: The determination of radionuclides and radiation levels in some of the most affected area of Fukushima, Japan (Lat. 37046N Long. 140028E) after the 2011 Tsunami employing the use of Radiagem 2000/Rados (RDS-31) dose rate meter for radiation survey measurement and hand held Hyper pure Germanium (HpGe) detector for in-situ Surface Concentration (SC) measurements was the aim of this study. Six (6) different locations were measured and analyzed, Insitu surface concentration measurements prominently of ^{134}Cs at energies 569, 605 & 796 keV and ^{137}Cs at energy 662 keV were established with little radiation from NORM alongside with dose rate measurement at the same locations. The ability of the detector to measure a Minimum Detectable Activity (MDA) as low as (0.10±0.02) Bqm^{-2} from a background area of about 400 m^2 established 95% of confidence limit on detection before commencing the Insitu measurements. The ranges of Insitu SC measurements for ^{134}Cs and ^{137}Cs for the Locations were found to be (162.11±0.46–59,649.39±6.61) Bqm^{-2} and Dose Rate measurements for the same locations were found to be (0.87±0.03–22.84±1.26) μSvh^{-1}respectively. The presence of ^{134}Cs and ^{137}Cs in these locations of Fukushima Prefecture, Japan showed an evidence of the nuclear accident as a result of the Tsunami disaster. The radiation levels recorded during the monitoring exercise was above the value of 0.2 μSvh^{-1} which Japanese Government hopes to achieve at the end of it ongoing environmental remediation before re-habitation of it evacuated citizens.

Key words: radiological monitoring, radiation, environment, fukushima

1. Introduction

On March 11, 2011, a 15 metre tsunami disable the power supply and cooling of three Fukushima Daiichi reactors as a result of foremost earthquake which led to largely melting of all the three cores within few days. This accident led to the discharged of several amounts of radioactive materials / fission products in the fuel to the environment causing the radiation level to rise above levels expected for human habitation that resulted in the evacuation of over 100,000 residents of the area within 20-30 km from the Nuclear Power Plant (NPP) with a criterion of 20 mSv/yr [1]. The radioactive materials / fission products released to the environment were majorly of Iodine-131 (^{131}I) with half-life of 8 days, Caesium-134 (^{134}Cs) with half-life of 2.5 years, Caesium-137 (^{137}Cs) with half-life of 30.07 years etc. which were easily carried from the plume resulting in land contamination [I]. Therefore out of these fission products, Caesium presently remains the major concern in the environment because of its yield and longer half- life.

Caesium is a metal that may be nonradioactive or radioactive, found in the alkali group of the periodic table. Caesium undergoes beta decay (β−) and is also a strong emitter of gamma radiation. It can easily be taken up by the body without concentrating in any particular organ with a biological half-life of 70 days. Dust particles contaminated by Cs may become air-borne and inhalation of contaminated dust can result in an internal exposure. Radiation from the radionuclides damages the body's soft tissues upon ingestion or inhalation as it is distributed evenly in the

Corresponding author: Godwin Ekong, MSc., research areas/interests: radiological monitoring, environment. E-mail: gobass04@yahoo.com.

body [1, 2]. Slightly higher concentrations of Cs are found in muscle, while slightly lower concentrations are found in bone and fat.

The most common radioactive form of Cs is ^{137}Cs which is more significant as an environmental contaminant than ^{134}Cs with its lower yield and shorter half-life. The primary source of ^{137}Cs in the biosphere is from atmospheric nuclear weapons testing from the 1940s to the 1960s where about 90% of ^{137}Cs was produced by atmospheric testing, 6% was created by the Chernobyl accident and 4% by nuclear fuel reprocessing facilities [3], which was dispersed and deposited all over the world and the accident at Chernobyl Although natural radionuclides result in a relatively small amount of radiation dose.

Several radiation monitoring programmes has been instituted by nuclear Experts all over the globe with the host country playing the leading role and radiation monitoring points/stations set up since March 11, 2011 till date to ensure that accurate radiation level is constantly reported before and up till the end of remediation action before Return of Evacuees. A monitory exercise was conducted on 17-21 November 2014 for determination of radionuclides activity / surface concentration and radiation level of some locations of Fukushima Prefecture, Japan.

2. Survey Method

The survey/sampling methods employed may be categorized into probability and non-probability sampling. However, Non probability was employed during this radiation monitoring exercise because the survey points were picked in such a way that it does not have equal chances of other points being selected.

This was majorly Judgemental - visual, historical site use or pre-identifies areas having potential of higher radioactivity concentrations, according to IAEA-TECDOC-1415.

"However, although judgmental samples are not necessarily representative samples, in the sense that they represent the presence and concentration levels of the target analytes of the whole site, they are still intended to be representative of that sub-portion of the site being investigated" [4].

Six major locations were chosen where the monitoring exercise took place. Their results and discussions with respective coordinates are presented in Paragraph 5, Figs. 5 and 6.

3. Equipment Specification/Theory

Spectrometer–HpGe Handy GPD 25300 (Fig. 1a)

(1) Detector properties, including:

• Type - HPGe p-type. All data analysis of was done using WINSPEC software

• Cooling mechanism and Dewar-LN2. MCA Battery operation time — 20 hrs

• Resolution (FWHM) at normal operation at 122–0.58 keV

(2) Calibration procedures and parameters were obtained using TECDOC 1092 and stepwise given below [5]:

- Certified reference point sources with a reasonably long half-life, having gamma line(s) in the medium energy range (58 keV line of Am-241, 122 keV line of Co-57, 662 keV line of Cs-137 and 1173 & 1332 keV of Co-60 were considered as good choices).
- The angular correction factor (Rf/Ro) for germanium detectors with comparable diameter and length was taken to be close to 1
- The geometrical factor (θ/As) was determined for the energy of interest from Fig. 1b
- Response factor (R0/Ø) was determined for this lines by following steps 3.1 to 3.5 in Procedure Dla uncollided flux (Ø) was determined from step 3 of D1a and measured corrected count rate (R0) for 120 seconds from the counter, A plot of response factor (R0/Ø) as a function of Energy (keV) gave the efficiency calibration which corresponds to that obtained in Fig. 2
- Parameters listed above [Geometrical factor (θ/As), Response factor (R0/Ø) and Angular correction

factor (Rf/Ro)] were therefore used to determined the Calibration Factor (Cf) given below:

$$\mathbf{Cf} = (\mathbf{R0}/\emptyset) * (\boldsymbol{\theta}/\mathbf{As}) * (\mathbf{Rf}/\mathbf{Ro}) \quad (1)$$

A plot of *Cf* as a function of energy (E) determined the efficiency (εff_{ab}) of the counter as shown in Fig. 2 below which is designated in Eq. (2) as G.

Please note that the efficiency (*G)* of energy (*E)* which lies between two measured energies of E_1 and E_2 with efficiencies G_1 and G_2 could be then calculated where required using linear interpolation as given below [6].

$$\boldsymbol{G} = \boldsymbol{G_1} + (\boldsymbol{G_2} - \boldsymbol{G_1})\frac{(\boldsymbol{E}-\boldsymbol{E_1})}{(\boldsymbol{E_2}-\boldsymbol{E_1})} \quad (2)$$

It is relevant to note that when $E = E_1$ this correctly gives the efficiency G_1 and that when $E = E_2$ it correctly gives the efficiency G_2. This is more precise than simply averaging G_1 and G_2 because averaging only applies to mid-point of interval of E_1 and E_2.

- Calibration full energy efficiency:
  - Efficiencies and (preferably) uncertainties for energies

Efficiency of 4.27±1.17 for Energy 88 keV, Efficiency of 4.15±0.64 for 122 keV, Efficiency of 3.20±0.53 for Energy 166 keV Efficiency of 1.82±0.22 for Energy 662 keV, Efficiency 1.12±0.10 for Energy 1173 keV and Efficiency of 1.12±0.10 for 1332 keV.

The value of efficiency (εff_{ab}) rose steadily where the photoelectric effect is considered to be dominant, requiring a few millimetres depth of the detector window for photon interactions and This efficiency curve conformed to that obtained from other studies [7, 8].

- Description of calibration efficiency geometry;

Crystal shape of detector sensitive area is 500 mm^2 while the sensitive region thickness — 14 mm and thickness of input window Al 0.5 mm, therefore approximately 3 cm distance between the detector cap and source/sample were observed for all dimensions measurements. This was taken in consistence with same distance applied in plume survey in Procedure A1.

- Energy calibration:

Channel 147 for Energy 88 keV, Channel 204 for 122 keV, Channel 276 for 166 keV, Channel 1337 for Energy 662 keV, Channel 1933 for Energy 1173 keV and Channel 2194 for 1332 keV as given in the system equation below:

$$E = 0.609\,keV/Ch * N - 3.091\,keV + 0.000E + 0\,keV/Ch^2 * N^2 \quad (3)$$

- FWHM versus energy:

FWHM of 1.6 keV for 88 keV, FWHM of 1.32 keV for 122 keV, FWHM of 1.12 keV for 662 keV, FWHM of 1.30 keV for 1173 keV, FWHM of 1.50 keV for 1332 keV

- From Eq. (1), S_C can be calculated thus [5]:

$$\boldsymbol{S_c} = \frac{\mathbf{10}\ \boldsymbol{X}\ \boldsymbol{N_{count}}}{\mathbf{C_f} \times \mathbf{I\gamma} \times \mathbf{t}} \quad (4)$$

Where N is net count, C_f is the calibration factor earlier determined, $I\gamma$ is absolute gamma decay intensity of the specific energy peak [IX] (also known as the emission probability per transformation for a specific energy photo peak) and t is the time of counts. Its unit of activity concentration is Bqm^{-2}.

4. Results

Data acquired from the spectrum during the Insitu measurement was done using WINSPEC software. The HpGe was held with maximum orientation of 0°-20° (see Fig. 1b) and at 1 m from the ground. The time of spectra acquisition was kept at 120 seconds throughout the monitoring exercise considering the high level of radioactivity in the environment. The S_C was calculated using Eq. (4) taking into account all the prominent multiple energy lines of each ^{134}Cs at 605 keV, 795 keV etc and ^{137}Cs at 662 keV as shown in Fig. 3.

The results of the S_c evaluated from acquired spectrum for the Insitu and dose rate measurement are presented in Table 1.

(a)

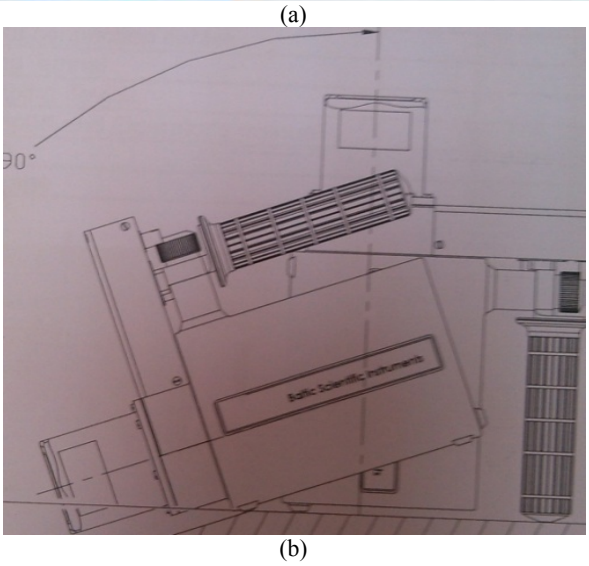

(b)

Fig. 1 (a) Showing Picture of HpGe Handy GPD 25300 system setup and (b) Schematic with 20 degrees of orientation without tripod. (Curled from the manufacturer's manual).

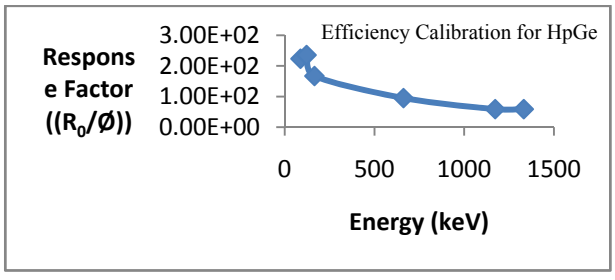

Fig. 2 Plot of C_f as a function of energy (E) determined the efficiency of the counter.

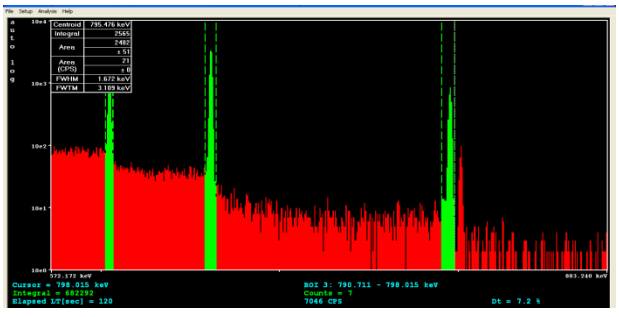

Fig. 3 Acquired Spectrums indicating energy lines of Cs-134 at 605 keV and 795keV, Cs-137 at 662 keV obtained during the insitu monitoring.

5. Discussion

The presence of ^{134}Cs and ^{137}Cs and high radiation dose rates in the six (6) locations of monitored showed the evident of nuclear accident resulting from Tsunami disaster where these radionuclides were discharge to the environment. The level measured was higher than that of exemption of bulk amount and clearance of solid material without further consideration for ^{137}Cs is 0.1 Bg/g which poses appreciable risk to the environment [9]. Fig. 4 affirmed the fact that the most common radioactive form of Caesium is ^{137}Cs which is much more significant as an environmental contaminant than the fairly common ^{134}Cs. This was evident in their percentage contribution where ^{137}Cs contributed 68.7% of environmental contamination as against 31.3% contribution of ^{134}Cs.

Dose Rate measurement for six (6) monitored locations is shown in Fig.5. The ranges of Dose Rate measured values were observed to be (0.87±0.03–22.84±1.26) μ Svh^{-1}, lower Dose Rate values indicted areas where environmental remediation had commenced while higher Dose Rate values as shown in the legend indicated areas observed to be the direction of the plume and where environmental remediation are yet to commenced or the primary spot of the disaster where the NPP is locate.

Insitu S_C (Bqm^{-2}) measurement for six (6) monitored locations is shown in Figure 6. The ranges of measured Insitu S_C values were observed to be (162.11±0.46–59,649.39±6.61) Bqm^{-2}. As noted earlier in Dose Rate measurements, lower values indicted areas where

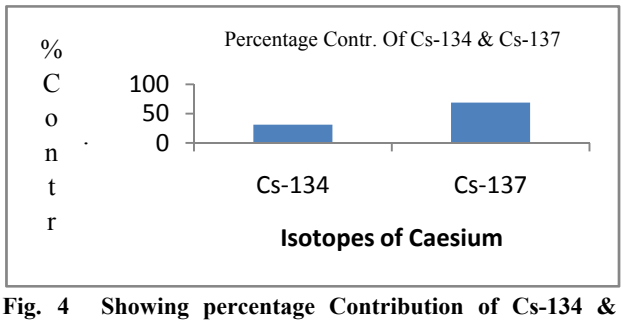

Fig. 4 Showing percentage Contribution of Cs-134 & Cs-137 contamination of the environment.

environmental remediation had commenced while higher values as shown in the legend indicated areas observed to be the direction of the plume, low plain regions and where environmental remediation are yet to commenced or the primary spot of the disaster where the NPP is locate.

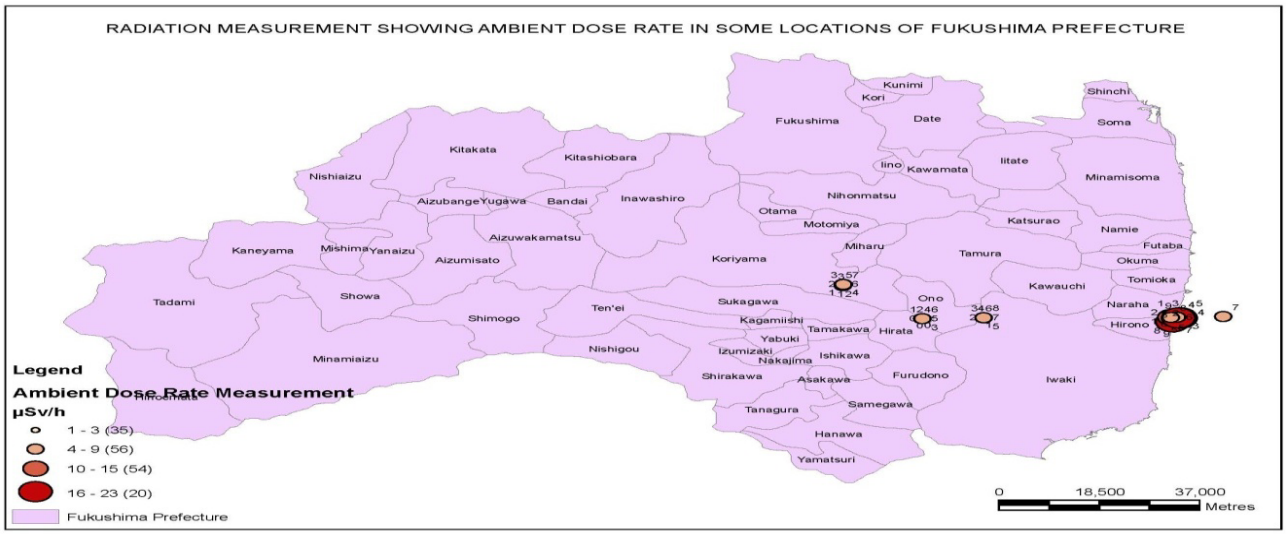

Fig. 5 Ambient Dose Rate (µSvh^{-1}) measurement for six (6) locations.

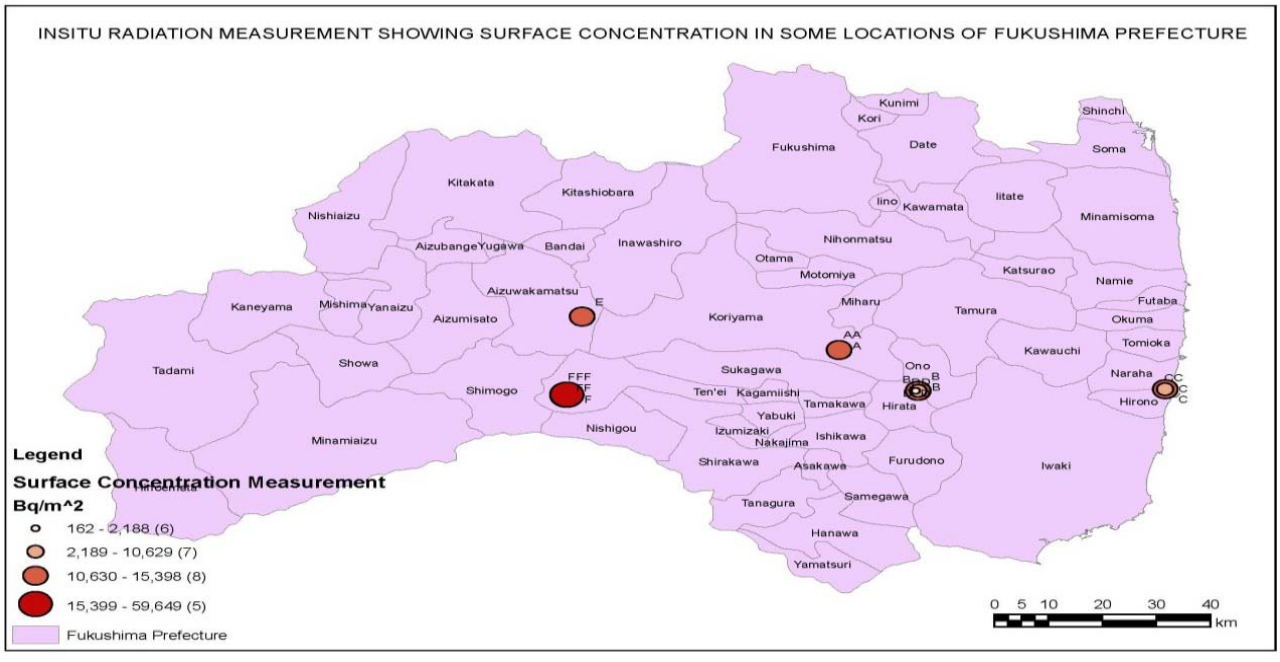

Fig. 6 Insitu surface concentration (Bqm^{-2}) measurement for six (6) locations.

The radiation levels recorded during the monitoring exercise exceeds recommended level as contained in ICRP publication 103 of 2007 where there is likelihood of resulting consequences of increased radiation exposures of both humans and other biota through various pathways. It is pertinent to note the evacuation in these areas of Fukushima has been effected and Japanese Government hopes to achieve at the end of environmental remediation a dose rate value of 0.2 μSvh^{-1} before resettlement of evacuated citizens.

6. Recommendation

Base on the monitoring result, it is recommended that periodic environmental monitoring be maintained to ensure that recommended dose rate is achieved before re-habitation.

7. Conclusion

Environmental monitoring exercise was carried out in the six (6) locations of Fukushima, Japan to determine dose rate level and of major radionuclide contaminant in the area. The result showed high level of radiation above habitable level in area under survey with the presence of ^{134}Cs and ^{137}Cs appearing as major contaminants also with minute traces of NORMs. ^{137}Cs was seen to be major contaminant to the environment than ^{134}Cs. Therefore, intensive cleanup and periodic environmental monitoring exercises is required until the area become habitable again in future.

Acknowledgement

Special gratitude to Incidence and Emergency Centre, International Atomic Energy Agency (IEC, IAEA) for putting up the Response and Assistance Network (RANET) workshop November 2014 and providing the funding to enable effective participation for the workshop.

Also, our thanks to the Japanese Government for permitting entry as well as playing a good host to the participant throughout the period of the exercise. Finally, the Nigerian Nuclear Regulatory Authority (NNRA) — our employer, granting approval and affecting our prompt release is deeply appreciated.

References

[1] Fukushima Accident – World Nuclear Association – www.world-nuclear.org/.../ Fukushima Accident. Last accessed January 9, 2015

[2] National Council on Radiation Protection and Measurements (NCRP), Cesium-137 in the environment: radioecology and approaches to assessment and management: recommendations of the National Council on Radiation Protection and Measurements, November 21, 2006, NCRP Report no.154, Bethesda, Md., 2007, ISBN: 9780929600918.

[3] US Environmental Protection Agency. (2012) 'Caesium'. Available at: http://epa.gov/rpdweb00/radionuclides/cesium.html. Accessed: 22nd December 2014.

[4] IAEA-TECDOC-1415

[5] Generic procedures for monitoring in a nuclear or radiological emergency, IAEA - TECDOC – 1092

[6] Thorne etal 2012, Thorne, M., Balding D., Egan, R., Paulley, A. LLWR Radiological Handbook; LLWR Environmental Safety Case Project, 2012, LLWR/ESC/R(10)10033 Issue 1.4

[7] Knoll, G. F., Radiation detection and measurement, 4thed,New York: John Wiley & Sons, 2010

[8] Al‐Sulaiti, H., Determination of Natural Radioactivity Levels of the State of Qatar Using High‐Resolution Gamma‐ray Spectrometry. MPhil to PhD Transfer Report, 2009 Department of Physics (University of Surrey).

[9] Update of X Ray and Gamma Ray Decay Data Standards for Detector Calibration and other Applications, International Atomic Energy Agency, Vienna, Austria. Volume 1, ISBN 92-0-113606-4.

[10] IAEA General Safety Requirement Part 3 Pp.126

Table 1 Result of insitu surface concentration measurement

Location	Coordinates	Radionuclide	Energy (Kev)	Dose Rate (uSv/h) with rados (RDS- 31)	Surface Concentration (Bq/m^2) (Surface)
Location B-G	Lat. 37 24329 Long. 140 58808	Cs-134	569	1.73±0.03	2187.62±3.61
		Cs-137	662		1306.38±0.83
		Cs-134	795		492.44±0.62
Location B-F	Lat. 37 24337 Long. 140 58815	Cs-134	605	0.97±0.02	224.47±0.62
		Cs-137	662		815.84
Location B-I	Lat. 37 24351 Long. 140 58822	Cs-134	605	0.87±0.03	162.11±0.46
		Cs-137	662		722.90±0.57
Location B-E	Lat. 37 24338 Long. 140 58816	Cs-134	605	1.03±0.04	324.23±0.62
		Cs-137	662		893.30±0.46
Location B-H	Lat. 37 24364 Long. 140 58828	Cs-134	605	1.03±0.02	207.84±0.42
		Cs-137	662		438.90±0.52
Location B-D	Lat. 37 24331 Long. 140 58820	Cs-134	605	1.37±0.02	324.23±0.54
		Cs-137	662		805.51±0.67
Location E- 001	Lat. 37 40873 Long. 140 03253	Cs-134	605	22.84±1.26	15180.58±3.78
		Cs-137	662		47127.77±5.42
		Cs-134	795		14908.58±3.36
Location E- 001(A)	Lat. 37 23460 Long. 140 00699	Cs-134	605	13.11±0.56	9169.87±3.91
		Cs-137	662		33965.87±5.42
		Cs-134	795		10070.74±2.81
Location E- 002(B)	Lat. 37 23445 Long. 140 00668	Cs-137	662	13.91±0.51	39289.49±5.83
		Cs-134	795		12213.68±2.81
LOCATION E-003(C)	Lat. 37 23435 Long. 140 00700	Cs-137	662	14.42±0.65	48852.40±6.35
		Cs-134	795		14843.65±3.19
Location E-004(D)	Lat. 37 23462 Long. 140 00711	Cs-134	605	11.64±1.13	34896.21±5.73
		Cs-137	662		43348.05±5.73
Location E-005(E)	Lat. 37 23463 Long. 140 00725	Cs-137	662	14.15±0.83	30320.40±4.85
		Cs-134	795		8528.47±2.49
Location E-006(F)	Lat. 37 23461 Long. 140 00738	Cs-137	662	14.30±0.70	59649.39±6.61
		Cs-134	795		17895.71±3.57
11					

Location A-001	Lat. 37 334500 Long. 140 4606	Cs-134	569	5.34±0.65	13805.38±14.87
		Cs-137	662		26716.23±4.08
Location A-002	Lat. 37 334490 Long. 140 4606	Cs-134	569	6.3±0.45	12913.34±14.02
		Cs-137	662		25600.91±4.03
Location A-003	Lat. 37 334400 Long. 140 4606	Cs-134	569	6.62±0.40	15398.31±15.29
		Cs-137	662		13781.53±4.44
Location B-001	Lat. 37 24325 Long. 140 59235	Cs-134	569	7.64±0.60	10364.65±7.86
		Cs-134	605		14548.75±4.41
		Cs-137	662		44267.16±5.32
Location B-002	Lat. 37 24323 Long. 140 59235	Cs-134	569	6.3±0.45	12913.34±14.02
		Cs-137	662		25600.91±4.03
Location B-003	Lat. 37 24318 Long. 140 59226	Cs-134	569	5.87±0.55	8686.77±10.83
		Cs-137	662		19585.37±3.51
Location B-004	Lat. 37 24325 Long. 140 59218	Cs-134	569	6.62±0.65	15398.31±15.29
		Cs-137	662		13781.53±4.44
Location B-005	Lat. 37 24318 Long. 140 59217	Cs-134	569	6.64±0.50	7093.84±10.19
		Cs-137	662		13404.59±2.84
Location B-006	Lat. 37 24319 Long. 140 59226	Cs-134	569	5.00±0.55	6477.91±11.47
		Cs-137	662		15697.21±3.20
Location C-001	Lat. 37 24677 Long. 141 00373	Cs-134	569	4.29±0.50	12446.08±11.47
		Cs-137	662		26711.07±4.08
Location C-002	Lat. 37 24678	Cs-134	605	3.09±0.45	10628.90±3.70
	Long. 141 00371	Cs-137	662		32163.79±4.44
Location C-003	Lat. 37 24698 Long. 141 00369	Cs-134	569	3.29±0.45	12700.95±18.69
		Cs-137	662		26835.00±4.08
Location C-004	Lat. 37 24697 Long. 141 00355	Cs-134	605	4.53±0.55	5748.83±3.08
		Cs-137	662		19585.37±4.03
		Cs-134	795		5627.92±4.09